Analyzing Lidar Observations over McMurdo, Antarctica to Investigate Vertical Development of Gravity Wave Energy in the Stratosphere and Mesosphere

Jackson Jandreau and Xinzhao Chu, *CIRES*, *CU Boulder*

Background

Lidar Observations of gravity waves have been made over McMurdo Station, Antarctica near-continuously since 2010. Lidar can measure waves in a wide spectra from diurnal tides to turbulence, enabling a range of studies. A major challenge of lidar GW studies is that shot-noise in the photon counting process strongly biases second-order parameters, complicating results.

$$Var(T') = \overline{(T'_{Wave})^2} + \overline{2T'_{Wave}T'_{Noise}} + \overline{(T'_{Noise})^2}$$

$$Cov(T'_{even}, T'_{odd}) = \overline{T'_{odd,Wave} * T'_{even,Wave}} + \overline{T'_{odd,Wave}T'_{even,Noise}} + \overline{T'_{even,Wave}T'_{odd,Noise}} + \overline{T'_{odd,Noise} * T'_{even,Noise}}$$

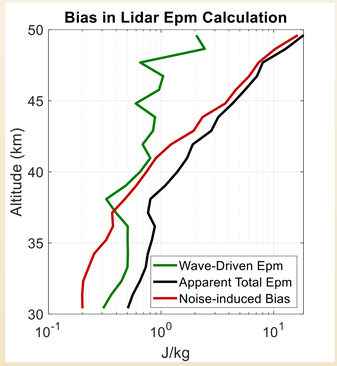

Above: Demonstration of second-order parameter bias
Left: Arrival Heights Observatory, McMurdo, Antarctica

Recently developed techniques (Gardner and Chu, 2020) pose a solution to this problem, eliminating the bias by subsampling the data into two unique sets and replacing **variance** with **covariance**. Due to uncorrelation in the noise-variance, these bias terms drop, leaving only wave energy.

Application

Gravity wave potential energy mass density (Epm) is used to estimate wave strength. It can be used to calculate momentum flux, observe secondary gravity-waves, and can be calculated easily using atmospheric temperature variance. Plotted as a dashed black line is the adiabatic growth rate of the Epm (its slope is relevant, not its absolute value).

These profiles are assembled from conservatively screened data from 2010-2020, where these means are weighted by observation length. The dashed line are a fit of the form $A \cdot \exp(b \cdot x)$ intended to illustrate general trends but not to characterize any physical mechanism other than general amplitude of the season's Epm.

$$Epm(z) = \frac{1}{2}\frac{g^2}{N^2}\overline{\left(\frac{T - T_0}{T_0}\right)^2}$$

This plot shows clear seasonal trends in the Rayleigh region: high winter Epm and low Summer Epm. The Epm grows at a relatively consistent rate year-round on average, with no major features present anywhere.

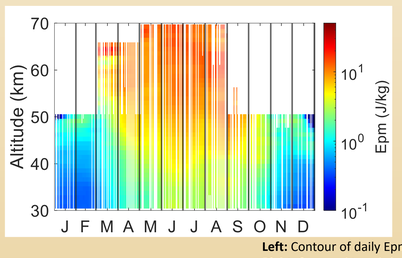

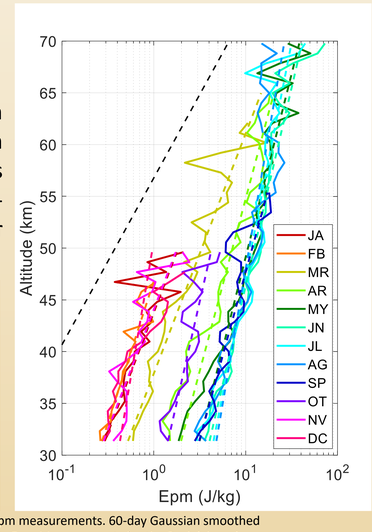

Left: Contour of daily Epm measurements. 60-day Gaussian smoothed
Right: Seasonal trends in Epm Measurements for the Rayleigh region

Here, the Rayleigh winter is replotted alongside the MLT winter. Generally, the Rayleigh Epm grows directly into the MLT Epm. Previous studies of this data suggested strong a dissipation source between the two, but new processing methods changed this.

Both regions generally showcase consistent dissipation (compared to the slope of the dashed black line), yet MLT Aug. and the upper Rayleigh may disagree slightly.

However, averaging smoothes out many features, so we must look at individual observations to interpret these plots (see below).

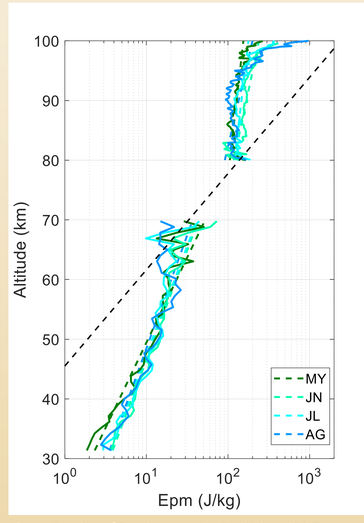

Above: Coupling of Epm between the Rayleigh and MLT regions

Data

- Observations made by Chu Group's Fe Boltzmann Lidar
  - Uses Rayleigh scattering products from 30-70 km
  - Uses resonance-fluorescence for 80-120km
- Rayleigh region processing
  - Processed as 1 km vertical bins, and 2 hr time bins with a step size of 1 hr
- Mesosphere-lower-thermosphere (MLT) processing
  - Processed as 0.5 km bins in 0.1 km steps and 15min bins in 6 min steps
- Data is split to 12-17 hr segments, with a minimum of 6 hr.

Rayleigh Region
Wavelength (km): 2-30
Period (hr): 4-11

MLT Region
Wavelength (km): 1-30
Period (hr): 0.5-11

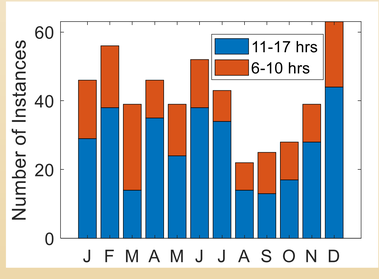

Right: Observation statistics from 2011-2020 for data shown in poster

Case Studies

Examination of single runs has results which generally agree with the trends above. What is absent from those trends are distinct regions of dissipation and growth. The exact cause for these regions is difficult to determine.

Both small dips in Epm and changes in its growth rate are present in the samples, as can be seen when compared with the adiabatic growth rate (dashed line).

These could be due to local dissipation/breaking but also could be waves entering or leaving the lidar's limited FOV. Longer runs minimize possibility of the latter.

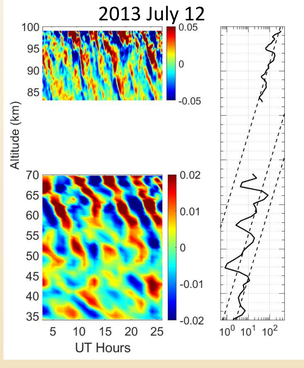

This run exhibits a few distinct regions of quasi-adiabatic growth, with each displaying some dissipation between them. Additionally, the Rayleigh Epm decreases briefly at the top of its window. The MLT profile is unremarkable here.

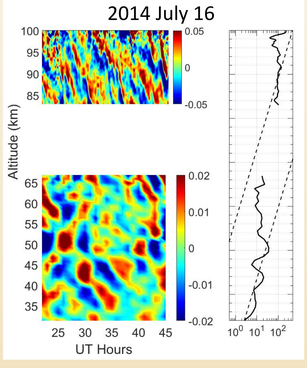

Rayleigh Epm begins with quasi-adiabatic growth aside from a few dips, followed by a wide region of decrease wave strength. This decrease can be seen in the Rayleigh contour as well. The MLT region grows adiabatically and then similarly decreases.

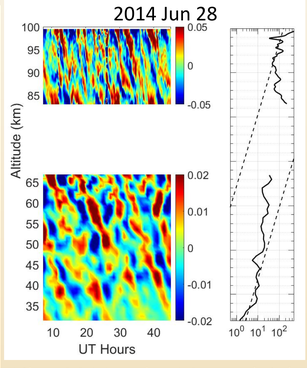

Like 2014 July 16, Rayleigh Epm grows adiabatically to a point, then its growth slows. In the lower MLT, the wave energy initially decreases and then begins to grow adiabatically or exceeds that rate. This is not uncommon with the MLT Epm.

Following Work

- Combine lidar data with satellite observations to determine seasonal momentum flux (MF) and wave propagation directions.
- Find more observations of secondary wave breaking present in data (prev. in Vadas et al. 2018) and assess their signature in Epm
- Assess spectra of upward and downward propagating MLT GW seen in the lidar data

Related Papers

Relevant to current work:

- Methodology - Jandreau and Chu, 2022
- Methodology - Gardner and Chu, 2020
- Methodology - Chu et al. 2018
- Data analysis - Lu et al. 2015
- GW Theory - Vadas et al. 2018

Relevant to future work:

- Alexander, 2010, 2015
- Chu et al. 2022 (unpublished)